

# Zinc Oxide Thin-Film Transistors with Location-Controlled Crystal Grains Fabricated by Low-Temperature Hydrothermal Method

Huang-Chung Cheng, Po-Yu Yang, Jyh-Liang Wang, Sanjay Agarwal,  
Wei-Chih Tsai, Shui-Jinn Wang, and I-Che Lee

**Abstract**—High-performance zinc oxide (ZnO) bottom-gate (BG) thin-film transistors (TFTs) with a single vertical grain boundary in the channel have been successfully fabricated by a novel low-temperature (i.e., 85 °C) hydrothermal method. The ZnO active channel was laterally grown with an aluminum-doped ZnO seed layer underneath the Ti/Pt film. Consequently, such BG-TFTs ( $W/L = 250 \mu\text{m}/10 \mu\text{m}$ ) demonstrated the high field-effect mobility of  $9.07 \text{ cm}^2/\text{V} \cdot \text{s}$ , low threshold voltage of 2.25 V, high on/off-current ratio above  $10^6$ , superior current drivability, indistinct hysteresis phenomenon, and small standard deviations among devices, attributed to the high-quality ZnO channel with the single grain boundary.

**Index Terms**—Hydrothermal method, lateral grain growth, thin-film transistor (TFT), zinc oxide (ZnO).

## I. INTRODUCTION

RECENTLY, zinc oxide (ZnO) as an active channel layer has been investigated for transparent thin-film transistors (TFTs) [1], [2] and compared with amorphous silicon TFTs [3] as well as organic TFTs [4]. The organic TFTs could be degraded in atmospheric conditions [4], and the amorphous silicon TFTs had some limitations in optical applications such as light sensitivity, light degradation, and opaqueness [3]. On the contrary, ZnO TFTs demonstrated not only high transparency but also relatively high field-effect mobility, less light sensitivity, and excellent chemical and thermal stability [5], indicating the potential of ZnO-based films in TFTs. The ZnO-based films have been prepared by various deposition techniques such as pulsed laser deposition, sputtering [1], atomic layer deposition [2], and chemical vapor deposition (CVD) [6], which usually suffered the following issues: high cost, low throughput, com-

Manuscript received November 30, 2010; accepted December 23, 2010. Date of publication February 14, 2011; date of current version March 23, 2011. This work was supported by the National Science Council of Taiwan under Contract NSC 99-2221-E-009-168-MY3. The review of this letter was arranged by Editor A. Nathan.

H.-C. Cheng, P.-Y. Yang, and I.-C. Lee are with the Department of Electronics Engineering and Institute of Electronics, National Chiao Tung University, Hsinchu 300, Taiwan (e-mail: youngboy.ee96g@g2.nctu.edu.tw).

J.-L. Wang is with the Department of Electronics Engineering, Ming Chi University of Technology, Taipei 243, Taiwan.

S. Agarwal is with the Department of Materials Science and Engineering, National Chiao Tung University, Hsinchu 300, Taiwan.

W.-C. Tsai is with the Department of Electronic Engineering, National Formosa University, Huwei 632, Taiwan.

S.-J. Wang is with the Institute of Microelectronics, Department of Electrical Engineering, National Cheng Kung University, Tainan 701, Taiwan.

Color versions of one or more of the figures in this letter are available online at <http://ieeexplore.ieee.org>.

Digital Object Identifier 10.1109/LED.2010.2103921

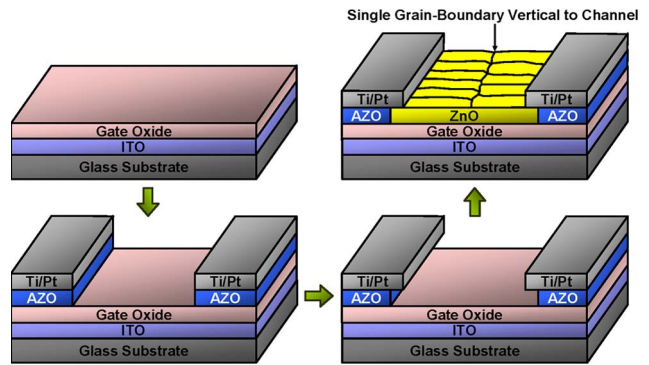


Fig. 1. Key process for fabricating location-controlled ZnO BG-TFT.

plicated operating conditions, and high energy consumption. In contrast, solution-based deposition processes, e.g., sol-gel process [7], chemical bath deposition [8], and aqueous solution-growth method [9], have offered comparatively simple, low cost, and large area thin-film deposition techniques. The presence of grain boundaries in the channel region of poly-ZnO TFTs has dramatic influence on the electrical characteristics. The localized potential barrier of grain boundaries retards the transportation of carriers from grain to grain [10]. Hence, enlarging the grain size improves the device performance effectively. To realize high-performance ZnO TFTs, it is essential not only to require larger grains but also to control the locations, number, and direction of grain boundaries in the ZnO active layer. In this letter, a simple low-temperature hydrothermal method was adopted to grow ZnO thin films. Moreover, the grain size and direction of grain boundaries in the ZnO active layer are designed with the technique of location-controlled nucleation at selected regions, and the related performance of fabricated ZnO TFTs is investigated.

## II. DEVICE STRUCTURE AND FABRICATION

Fig. 1 schematically shows the key process for the fabrication of hydrothermally grown ZnO bottom-gate (BG) TFTs with the technique of location-controlled nucleation. A 200-nm-thick indium tin oxide film was deposited by sputtering on the glass substrate and served as the gate electrode. After a cleaning process, a 200-nm-thick tetraethylorthosilicate silicon dioxide (TEOS-SiO<sub>2</sub>) layer as the gate dielectric was deposited by plasma-enhanced CVD at 350 °C. A sputtered aluminum-doped ZnO (AZO) film (200 nm) and Ti (100 nm)/Pt (50 nm) films were sequentially deposited at room temperature and patterned

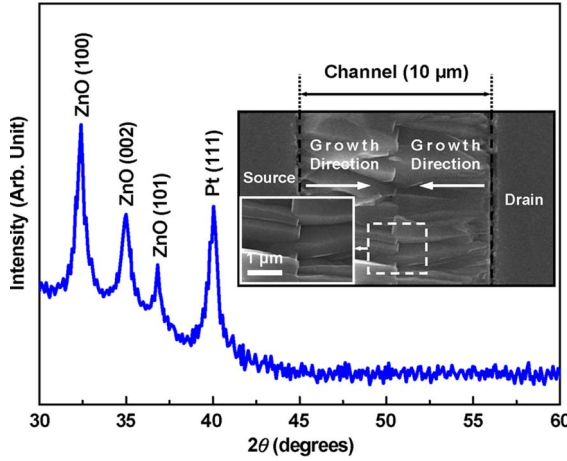


Fig. 2. XRD diffraction pattern of location-controlled ZnO BG-TFT. The inset shows the corresponding FE-SEM image.

by a lift-off process. Furthermore, the samples were dipped in 0.001-M phosphoric acid ( $H_3PO_4$ ) to undercut the AZO seed layer and then immersed in the hydrothermal solution to grow the ZnO film. The solution was prepared by mixing 0.25-M zinc nitrate hexahydrate ( $Zn(NO_3)_2 \cdot 6H_2O$ ) with 0.25-M hexamethylenetetramine in deionized water at 85 °C. Finally, the samples were annealed at 400 °C for 1 h in  $O_2$  ambience. After the TFT fabrication, a semiconductor parameter analyzer (4156C, Agilent Technologies) integrated with a probe station was used to measure the  $I-V$  characteristics. The crystal structure of the prepared devices was examined by an X-ray diffractometer (XRD, MAC science M18XHF) using the incident Cu  $K\alpha$  ( $\lambda = 0.154$  nm) radiation. The surface morphologies were observed by field-emission scanning electron microscopy (FE-SEM, Hitachi S-4700I). Analytical field-emission transmission electron microscopy (TEM, JEM-2100FX) was employed to analyze the microstructure and crystallinity of the ZnO films in the channel region.

### III. RESULTS AND DISCUSSION

Fig. 2 shows the XRD pattern of the location-controlled ZnO BG-TFT. The diffraction peaks (100), (002), and (101) indicated that the ZnO films have a hexagonal wurtzite structure. The Pt (111) peak was sourced from the Pt electrode. The inset in Fig. 2 shows the corresponding FE-SEM image, which revealed that the lateral grain growth started from the edges of the AZO seed layer beneath the underlayered Ti/Pt film and extended toward the middle of the channel from both sides in the opposite direction. The lateral size of the grains was about 5  $\mu m$  while the distance between the source and drain was 10  $\mu m$ . Fig. 3 shows the cross-sectional TEM image, high-resolution TEM (HRTEM) image, and corresponding selected-area electron diffraction (SAED) patterns of the 200-nm-thick ZnO film with the BG structure. There were two large ZnO grains formed and impinged with each other, while the vertical grain boundary was artificially controlled in the middle of the channel region above the BG electrode. It is evident that the location-controlled lateral grains collided at the middle of the channel, resulting in only a single grain boundary perpendicular to the channel direction. The spot pattern of SAED (inset of the bottom image in Fig. 3) confirms that ZnO grains in

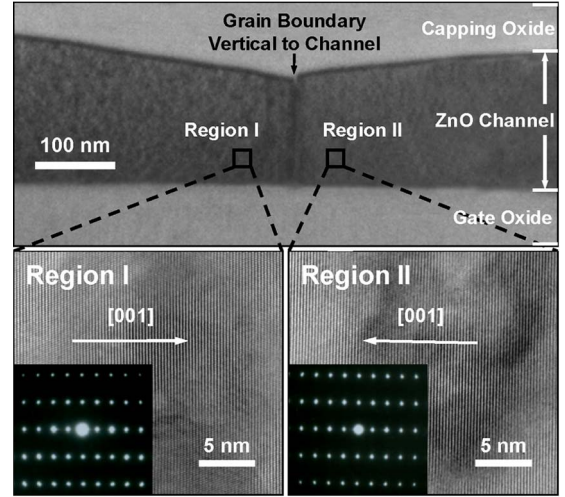


Fig. 3. (Top) Cross-sectional TEM image. (Bottom) HRTEM images and SAED patterns of location-controlled ZnO BG-TFT. The capping oxide layer was used to protect device structure from the bombardment damage induced by focused ion beam during TEM sample preparation.

the channel regions (regions I and II) were a single-crystalline wurtzite structure. Also, the HRTEM images have clearly revealed a well-resolved lattice image. Moreover, the orientation of the grain growth was along the [001] direction ( $c$ -axis of the ZnO crystal) which was the fastest growth direction of ZnO crystals. The misfit angle of neighbor ZnO grains was found to be about 2.7°. The top image in Fig. 4 shows the transfer characteristics ( $I_{DS}-V_{GS}$  and  $I_{DS}^{1/2}-V_{GS}$  plots) for ZnO BG-TFTs. The positive gate voltage was applied to turn on the TFTs, which suggested the behavior of n-channel enhancement-mode devices. The gate leakage current ( $I_{GS}$ ) is less than 1 nA and is comparable with those of conventional sputtered ZnO TFTs [11]. The threshold voltage ( $V_{TH}$ ) and field-effect mobility ( $\mu_{FE}$ ) were extracted with a line fitting of the square root of  $I_{DS}-V_{GS}$  in the saturated current region [12]. The excellent  $\mu_{FE}$  of 9.07  $cm^2/V \cdot s$ , low  $V_{TH}$  of 2.25 V, and high on/off-current ratio (i.e., above  $10^6$ ) were achieved, which can be linked to the high-quality location-controlled ZnO films with the single vertical grain boundary in the channel region. It is well known that the grain boundary acts as a strong trapping center which degrades the performance of TFTs, resulting in an increase in  $V_{TH}$ , a decrease in  $\mu_{FE}$ , a rise in the leakage current, and poor stability [13]. The higher  $V_{TH}$  and lower  $\mu_{FE}$  represents more defects in the channel region which require the larger gate voltage in order to fill the number of trap states before the device can be turned on. After trapping free carriers in the grain boundaries, the defect states become electrically charged and create a potential energy barrier during carrier transport from the drain to the source [13]. The inset reveals the drain-current versus drain-voltage ( $I_{DS}-V_{DS}$ ) output characteristics. The drain current increased linearly with drain voltage at lower values, and saturation behavior was observed at high drain voltages due to the pinchoff effect by the accumulation layer. Furthermore, the excellent  $\mu_{FE}$  (i.e., 9.07  $cm^2/V \cdot s$ ) of hydrothermally grown ZnO BG-TFTs was a remarkable achievement as compared to those (i.e., 0.24–1.16  $cm^2/V \cdot s$ ) prepared by solution-based processes [7]–[9]. The bottom image in Fig. 4 shows a hysteresis phenomenon, the shift of threshold voltage ( $\Delta V_{TH}$ ), observed between the forward and

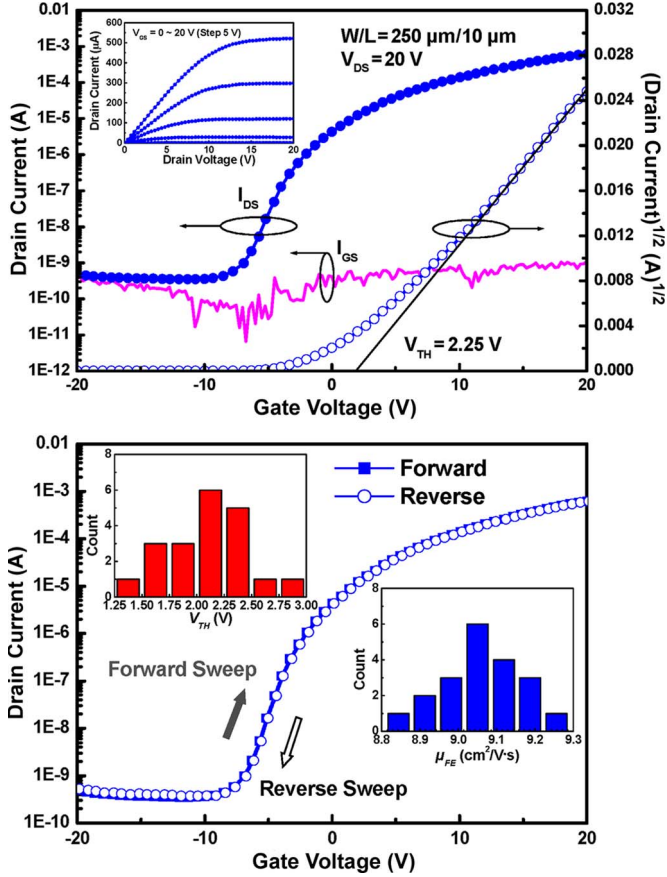


Fig. 4. (Top) Transfer characteristics ( $I_{DS}-V_{GS}$  and  $I_{DS}^{1/2}-V_{GS}$ ) and gate leakage current ( $I_{GS}$ ) of location-controlled hydrothermal ZnO BG-TFTs with the channel width ( $W$ ) of 250  $\mu\text{m}$  and channel length ( $L$ ) of 10  $\mu\text{m}$  at the drain voltage ( $V_{DS}$ ) of 20 V. Inset shows the output characteristics ( $I_{DS}-V_{DS}$ ). (Bottom) Forward and reverse sweeps in transfer characteristics, while the gate voltage swept from -20 to 20 V and 20 to -20 V, accordingly. Insets give statistical distributions of threshold voltage ( $V_{TH}$ ) and field-effect mobility ( $\mu_{FE}$ ) for 20 measured location-controlled ZnO BG-TFTs.

reverse gate voltage sweeps in the transfer characteristics. The calculated  $\Delta V_{TH} = 0.16$  V, and it is smaller than the reported values (i.e., 1–2.3 V) [14], [15]. The  $\Delta V_{TH}$  in the hysteresis loop is associated with the traps at the interfaces of the channel/dielectric or the gate electrode/dielectric. The slighter  $\Delta V_{TH}$  (indistinct hysteresis phenomenon) advises the fewer traps in the channel region owing to the single vertical small-angle grain boundary. The insets demonstrate the statistical distributions of  $V_{TH}$  and  $\mu_{FE}$  in the ranges of 1.25–3 V and 8.8–9.3  $\text{cm}^2/\text{V}\cdot\text{s}$  with normal distributions centered at 2.17 V and 9.05  $\text{cm}^2/\text{V}\cdot\text{s}$ , correspondingly. The proposed TFTs reveal the indistinct hysteresis phenomenon and small standard deviations among devices, indicating the improved stability and device-to-device uniformity. Briefly, the results suggest that the proposed hydrothermally grown ZnO BG-TFT with the single vertical small-angle grain boundary can contribute superior electrical characteristics.

#### IV. CONCLUSION

The laterally grown ZnO BG-TFTs were fabricated by a hydrothermal method on a glass substrate. The lateral grain

growth started from both sides of the AZO seed layers beneath the Ti/Pt films and extended toward the middle of the channel. The location-controlled lateral grain growth impinged at the middle of the channel, resulting in only a single grain boundary perpendicular to the channel direction. The superior device performance (i.e., the high  $\mu_{FE}$  of 9.07  $\text{cm}^2/\text{V}\cdot\text{s}$ , low  $V_{TH}$  of 2.25 V, and high on/off-current ratio above  $10^6$ ), indistinct hysteresis phenomenon, and small standard deviations among devices have been obtained for such ZnO BG-TFTs, which are attributed to the high-quality ZnO channel with the single grain boundary that has a misfit angle of 2.7°. Therefore, the proposed location-controlled hydrothermally grown ZnO BG-TFTs have revealed the potentials for future active matrix organic light-emitting diodes and system on panel.

#### REFERENCES

- [1] P. F. Garcia, R. S. McLean, M. H. Reilly, and G. Nunes, "Transparent ZnO thin-film transistor fabricated by rf magnetron sputtering," *Appl. Phys. Lett.*, vol. 82, no. 7, pp. 1117–1119, Feb. 2003.
- [2] P. F. Garcia, R. S. McLean, and M. H. Reilly, "High-performance ZnO thin-film transistors on gate dielectrics grown by atomic layer deposition," *Appl. Phys. Lett.*, vol. 88, no. 12, p. 123509, Mar. 2006.
- [3] D. L. Staebler and C. R. Wronski, "Reversible conductivity changes in discharge-produced amorphous Si," *Appl. Phys. Lett.*, vol. 31, no. 4, pp. 292–294, Aug. 1977.
- [4] H. E. Katz, J. Johnson, A. J. Lovinger, and W. Li, "Naphthalenetetracarboxylic diimide-based n-channel transistor semiconductors: Structural variation and thiol-enhanced gold contacts," *J. Amer. Chem. Soc.*, vol. 122, no. 32, pp. 7787–7792, Jul. 2000.
- [5] C. Y. Tsay, K. S. Fan, S. H. Chen, and C. H. Tsai, "Preparation and characterization of ZnO transparent semiconductor thin films by solgel method," *J. Alloys Compounds*, vol. 495, no. 1, pp. 126–130, Apr. 2010.
- [6] Y. Natsume, H. Sakata, and T. Hirayama, "Low-temperature electrical conductivity and optical absorption edge of ZnO films prepared by chemical vapour deposition," *Phys. Status Solidi (A)*, vol. 148, no. 2, pp. 485–495, Apr. 1995.
- [7] G. A. C. Jones, G. Xiong, and D. Anderson, "Fabrication of nanoscale ZnO field effect transistors using the functional precursor zinc neodecanoate directly as a negative electron beam lithography resist," *J. Vac. Sci. Technol. B, Microelectron. Nanometer Struct.*, vol. 27, no. 6, pp. 3164–3168, Nov. 2009.
- [8] H. C. Cheng, C. F. Chen, and C. C. Lee, "Thin-film transistors with active layers of zinc oxide (ZnO) fabricated by low-temperature chemical bath method," *Thin Solid Films*, vol. 498, no. 1/2, pp. 142–145, Mar. 2006.
- [9] C. Li, Y. Li, Y. Wu, B. S. Ong, and R. O. Loutfy, "ZnO field-effect transistors prepared by aqueous solution-growth ZnO crystal thin film," *J. Appl. Phys.*, vol. 102, no. 7, p. 076101, Oct. 2007.
- [10] F. M. Hossain, J. Nishii, S. Takagi, A. Ohtomo, T. Fukumura, H. Fujioka, H. Ohno, H. Koinuma, and M. Kawasaki, "Modeling and simulation of polycrystalline ZnO thin-film transistors," *J. Appl. Phys.*, vol. 94, no. 12, pp. 7768–7777, Dec. 2003.
- [11] C. C. Liu, Y. S. Chen, and J. J. Huang, "High-performance ZnO thin-film transistors fabricated at low temperature on glass substrates," *Electron. Lett.*, vol. 42, no. 14, pp. 824–825, Jul. 2006.
- [12] H. H. Hsieh and C. C. Wu, "Scaling behavior of ZnO transparent thin-film transistors," *Appl. Phys. Lett.*, vol. 89, no. 4, pp. 041109-1–041109-3, Jul. 2006.
- [13] G. Y. Yang, S. H. Hur, and C. H. Han, "A physical-based analytical turn-on model of polysilicon thin-film transistors for circuit simulation," *IEEE Trans. Electron Devices*, vol. 46, no. 1, pp. 165–172, Jan. 1999.
- [14] S. T. Meyers, J. T. Anderson, C. M. Hung, J. Thompson, J. F. Wager, and D. A. Keszler, "Aqueous inorganic inks for low-temperature fabrication of ZnO TFTs," *J. Amer. Chem. Soc.*, vol. 130, no. 51, pp. 17603–17609, Dec. 2008.
- [15] J. Nishii, F. M. Hossain, S. Takagi, T. Aita, K. Saikusa, Y. Ohmaki, I. Ohkubo, S. Kishimoto, A. Ohtomo, T. Fukumura, F. Matsukura, Y. Ohno, H. Koinuma, H. Ohno, and M. Kawasaki, "High mobility thin film transistors with transparent ZnO channels," *Jpn. J. Appl. Phys.*, vol. 42, no. 4A, pp. L347–L349, Apr. 2003.